Conference paper

Michail I. Alymov*, Boris S. Seplyarskii, Nickolai M. Rubtsov, Sergey G. Vadchenko, Roman A. Kochetkov, Nayil I. Abzalov and Ivan D. Kovalyov

Macrokinetic investigation of the interaction mechanism of the pyrophoric iron nanopowder compacts with air

https://doi.org/10.1515/pac-2019-1112

Abstract: It is shown that self-heating of a compacted sample made of nonpassivated iron nanopowder is not uniform, although it begins simultaneously within the entire surface of the sample. It is found that the maximum temperature of self-heating decreases with an increase in relative density of samples, which indicates that the oxidation process is limited by the diffusion supply of oxidant. It is shown that the process of interaction of samples with the air occurs in a superficial mode. A qualitative agreement of the results of the theoretical analysis with experimental data is obtained. The possibility of passivation of compacted samples made of iron nanopowder is experimentally established.

Keywords: air; compact samples; interaction; iron nanopowder; microstructure; Mendeleev-21; passivation; pyrophoricity; self-heating.

Introduction

Metal nanopowders are pyrophoric, i.e., these are capable of self-ignition upon contact with air due to high chemical activity and large specific surface area [1–4]. In order to make safe further processing of nanopowders, these are passivated [3–7]. The process of passivation is to create a thin protective film on the surfaces of nanoparticles, which prevents the self-ignition of metal nanopowders. The passivation of iron and nickel nanopowders was investigated in [8–11].

However, it is evident that there may be situations, in which it is technically impossible or undesirable to passivate the nanopowder, although technical operations with the nanopowder need to be carried out. Therefore, it is an urgent task to study both self-ignition and self-heating of compact products made of nanopowders to develop new methods of obtaining compact products from nanopowders, which ensure the required level of fire and explosion safety.

The literature on the features of self-ignition and self-heating of compacted samples made of nonpassivated nanopowders is quite limited. In the works [12, 13], ignition tests of nanosystems with a particle size of the reactants in the range of 40–80 nm showed that in these cases, the temperature and energy of ignition are considerably lower than in the mixtures of micro-particles (1–100 μm). In the work [14], the peculiarities of flame propagation over the tablets made of the mixtures of Al/CuO nanopowders (so-called nanothermites)

Article note: A collection of invited papers based on presentations at 21st Mendeleev Congress on General and Applied Chemistry (Mendeleev-21), held in Saint Petersburg, Russian Federation, 9-13 September 2019.

***Corresponding author: Michail I. Alymov**, Merzhanov Institute of Structural Macrokinetics and Materials Science, Russian Academy of Sciences, Chernogolovka, Russia, e-mail: alymov@ism.ac.ru

Boris S. Seplyarskii, Nickolai M. Rubtsov, Sergey G. Vadchenko, Roman A. Kochetkov, Nayil I. Abzalov and Ivan D. Kovalyov: Merzhanov Institute of Structural Macrokinetics and Materials Science, Russian Academy of Sciences, Chernogolovka, Russia

depending on the density at laser initiation of combustion were investigated. It was shown that less dense samples (90% porosity) ignited faster and the flame propagation velocity within them was an order of magnitude higher than in denser samples (50% porosity). These results, in the authors' view, indicate a change in the combustion mechanism from a convective to diffusion one with an increase in the density of a compacted sample. The measurements outlined in the monograph [15] were performed with the samples of Al/MoO_3 nanopowders; the results obtained for the nanothermite are qualitatively similar to those described in [14].

In the present work, macrokinetic modes (self-ignition or combustion) of the interaction of compact samples made of nonpassivated iron nanopowders with the air were revealed and investigated. The influence of the porosity of the compact samples on the dynamics of their self-heating has also been studied.

Experimental

Iron nanopowders obtained by a chemicometallurgical method were used for experimental studies of ignition and passivation of compact samples [6]. The main stages of synthesis of metallic nanopowders by this method are sedimentation of the metal hydroxide, its drying, reduction, and passivation. After synthesis, the nanopowders are pyrophoric. The average diameter of the nanoparticles calculated from the specific surface area of the powder was 85 nm.

Opening the vessels with nanopowders and all subsequent operations of weighing, pressing and measurement of sample sizes, were carried out in a sealed box (further box) filled with inert gas (argon) and equipped with scales, mold tools, measuring tools, a press and a lock for changing powders and samples (Fig. 1). The oxygen concentration in the box was monitored with the AKPM-1-02 analyzer. The concentration did not exceed 0.1 vol% at the opening of the powder vessels and during samples pressing. At that oxygen concentration, the nanopowders were pyrophoric. Cylindrical samples 5 mm in diameter, 7 ÷ 12 mm in length,

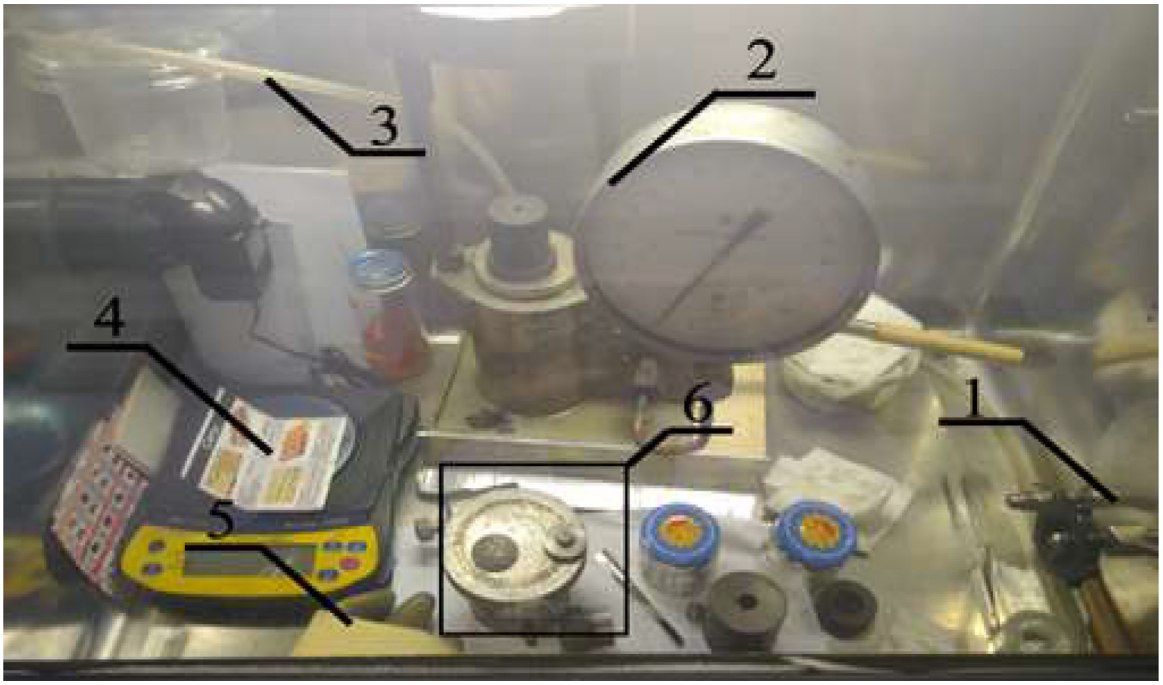

Fig. 1: General view of the installation for obtaining compact samples inside the sealed box: 1 – lock, 2 – press, 3 – output to the oxygen analyzer, 4 – digital scales, 5 – gloves, 6 – set of molds.

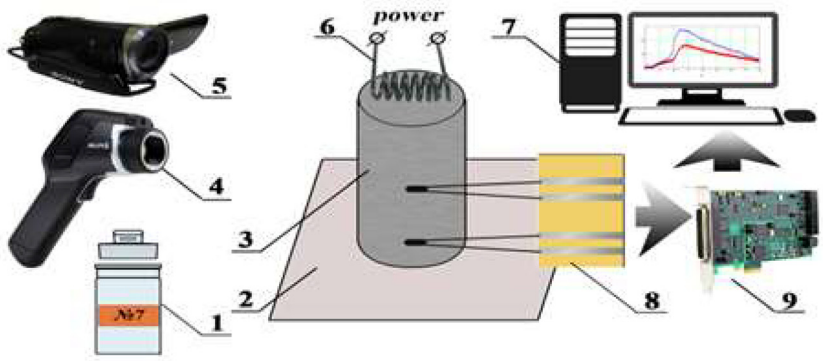

Fig. 2: The scheme of the experiment for studying the dynamics of sample heating in the air: 1 – weighing bottle with a compact sample after extraction from the box, 2 – boron nitride substrate, 3 – sample being tested, 4 – Flir E60 thermal imager, 5 – digital video camera, 6 – tungsten spiral, 7 – PC for data recording, 8 – contact platform with fixed thermocouples, 9 – ADC.

and 2.5 ÷ 4 g/cm^3 density made of iron nanopowder were obtained and examined. After pressing, each sample was placed in a separate weighing bottle and then removed from the box through a lock.

The study of heating, ignition and combustion of the samples was carried out in the air. The experimental design is presented in Fig. 2.

The samples were removed from the box and mounted vertically for a few seconds on a boron nitride stand. The measurements of the time dependence of temperature distribution over a sample surface, and the maximum temperature at the moment were carried out with a Flir 60 infrared camera (60 frames/s, 320 × 240 pix, sensitivity 8–14 μm). A SONY HDR-CX330 video camera was used to measure the combustion velocity (propagation of the oxidation reaction along the sample surface). The dynamics of temperature change within the sample surface was also controlled by two rolled 40 μm thermocouples, tightly touching the lateral surface of the sample. These were located a millimeter and 4 mm from the lower end of the sample.

Results and discussion

In order to check the preservation of pyrophoricity of nanopowder after manipulations in the box, a part of the powder was poured into a weighing bottle, which was opened after extraction from the box, and the powder was sprayed in the air. The powder ignited and burned brightly (see Fig. 3), thus, it remained pyrophoric for all preparatory operations.

In the first series of experiments, closed weighing bottles with samples after extraction from the box, until the beginning of the experiment, i.e., before extraction of the samples out of the weighing bottles, were kept in an argon atmosphere. In Fig. 4, the results of video filming of the self-heating process without the external initiation of a compacted sample made of pyrophoric iron nanopowder in the air are presented. This type of

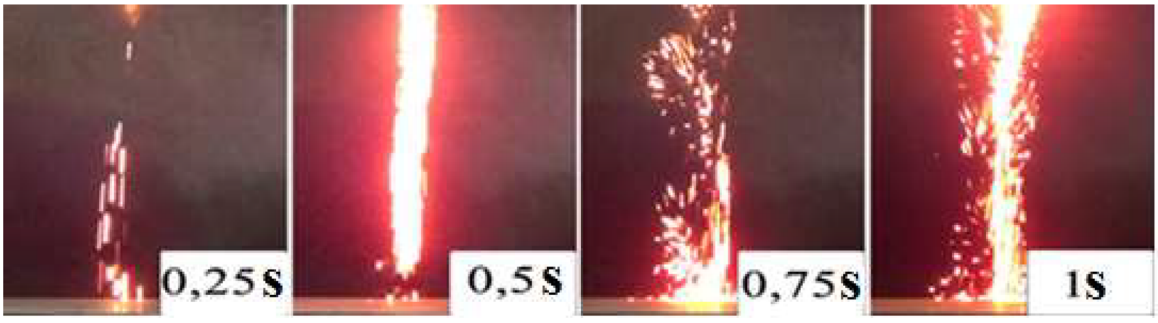

Fig. 3: Frames from video film of combustion of the initial sample of iron nanopowder in the air.

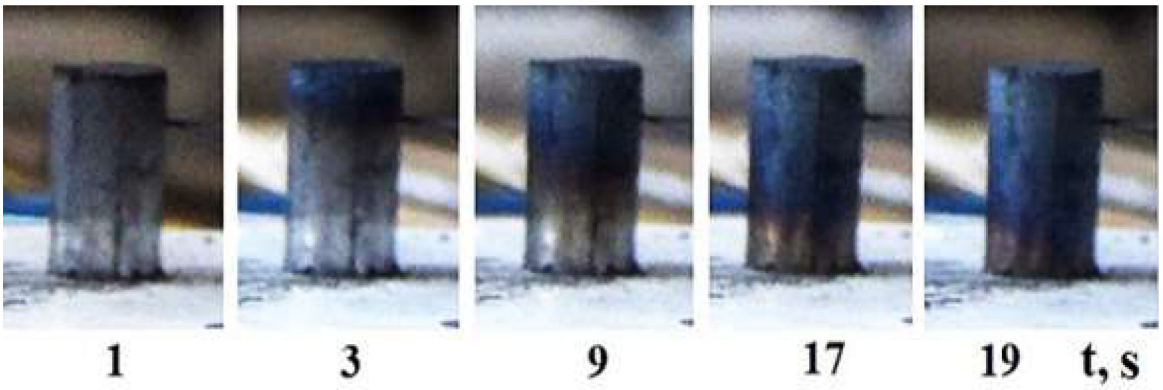

Fig. 4: Consecutive frames of video film of a compact sample during self-heating.

interaction with the air is observed for all samples, if the weighing bottles with those were stored before in argon atmosphere.

Notice that self-heating of the sample is non-uniform, although it begins simultaneously within the entire surface of the sample. This is evidenced by thermocouple measurement data (Fig. 5 curves 2,3) and infrared video film obtained by means of Flir – 60 (Fig. 5 curve 1).

As is seen in Fig. 5, the warming-up process, having started at the same time at different points of the sample, then occurs with different velocities, and various maximum temperatures are achieved during the heating. The reason for the non-uniformity of the sample heating is both the better conditions for the oxidant supply at the upper end (the lower end is placed on the gas-inpermeable substrate) and the heat losses into the massive substrate. Another reason for the non-uniformity of the heating is the inhomogeneity of the density of the sample with its height.

It is known that at pressing samples, the length of which exceeds the diameter by more than 2 times, non-uniformity of density and, therefore, porosity along the length of the compact can take place [16]. According to [16], the most dense part of the sample is located on the side of a movable (in our case upper) punch.

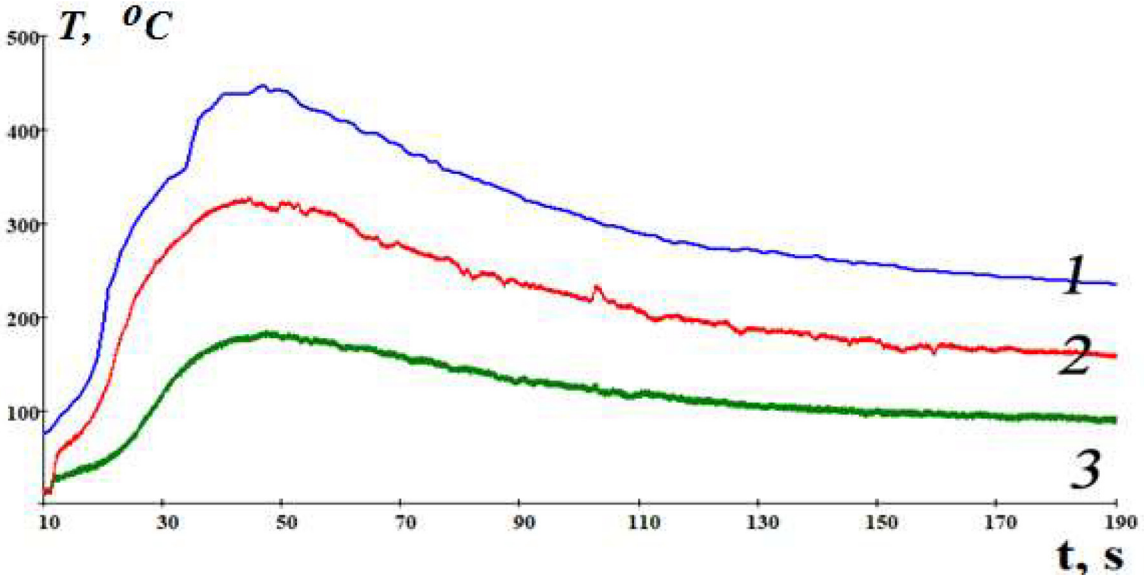

Fig. 5: Temperature changes with time at different points in the sample. 1 – data of infrared video framing, 2,3- thermocouple measurements.

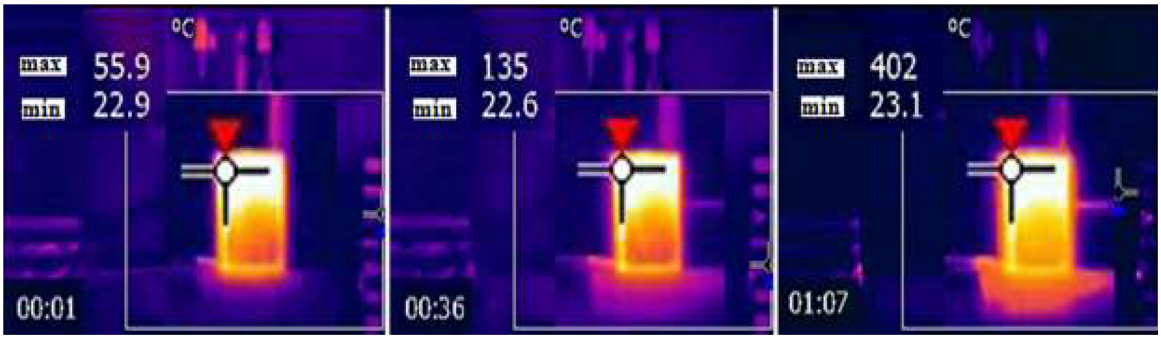

Fig. 6: Consecutive frames of IR video film of compact sample during self-heating.

Experiments showed that inhomogeneity of density affects the dynamics of heating pyrophoric samples. The difference between the density of the upper and lower end of the 5 mm diameter sample is 0.57 g/cm^3, i.e., 20% of the average density of the sample. The measurements were performed as follows: the sample was previously weighed on an analytical balance, and its length was measured with 0.1 mm accuracy, then the sample was fixed in a special shape and ground layer-by-layer. The weight and length of the remained sample were then fixed again and the density of the remote part of the sample was calculated.

Infrared video capture data showed that at almost all stages of the interaction, the maximum temperature was near the upper end of the sample (Fig. 6). For visual analysis of IR video film, it is necessary to consider the features of image processing by the Flir 60 infrared camera: the area with the maximum value of temperature at the moment has similar brightness for all frames at the given moment. The real values of the maximum and minimum temperature are shown near the left boundary of each frame. A bigger cross on an each frame specifies the selected point, in which the temperature is taken; the smaller cross automatically specifies a point with maximum temperature in a frame. The value of maximum temperature is shown at the top of the frame.

On the basis of data [8], it could be expected that the process of interaction of the sample with air is surface one; there remains unreacted nanopowder in the inner layers of the sample. To verify this assumption, the fracture of the sample after cooling was analyzed. Fig. 7 shows the photos of the fracture and a fragment of the sample fracture.

Two areas of different colors are visible in the sample fracture. The surface darker layer according to the X-ray phase analysis, as compared to the central region, contains a significant amount of iron oxides. These results directly indicate the superficial combustion mode of the sample. The thickness of the surface (oxidized) layer is about 0.35 mm.

Based on thermocouple measurements, it should also be noted that a decrease in the relative density of the samples from 3.84 g/cm^3 to 3.22 g/cm^3 results in an increase in the maximum self-heating temperature from 290 to 385 °C, indicating that the oxidation process is limited by the diffusion supply of the oxidant into the sample. These results are in qualitative agreement with theoretical analysis [8], according to which the maximum

Fig. 7: The appearance of a 5 mm diameter sample fracture after cooling. The photos were taken at different magnification.

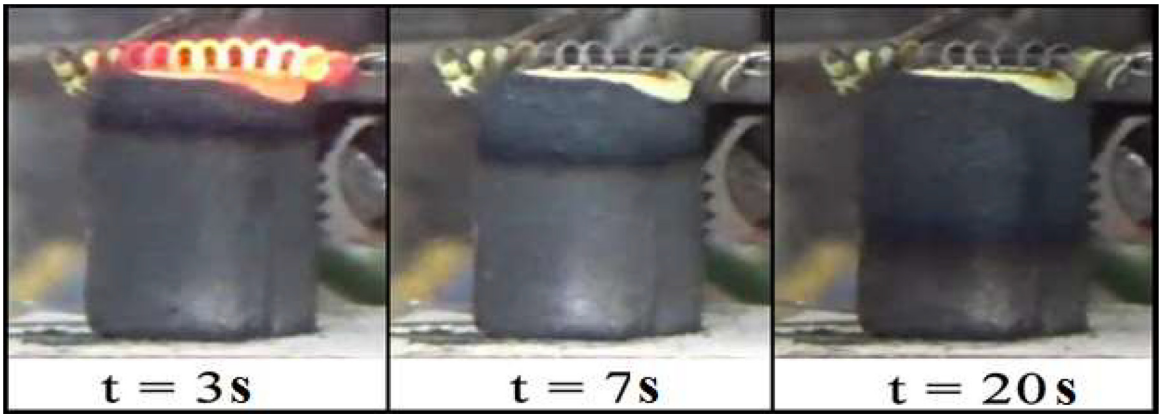

Fig. 8: Various frames of video film of the combustion of the sample, which was in the air for more than 20 min (density 3.07 g/cm^3).

temperature in the diffusion-controlled wave of conversion θ_{fr} depends on the governing parameters of the process as follows: $\theta_{fr} = \frac{\eta_{1,k}}{\gamma\nu} \Big/ \left(1 + \frac{\sqrt{2}}{\sqrt{\pi}} \frac{\sqrt{\eta_{1,k}}}{\sqrt{Le\nu}}\right)$

$$\theta = \frac{E}{RT_0^2}(T - T_0),\ \gamma = \frac{c_c RT_0^2}{EQ} \frac{\rho_c}{\rho_g a_0},\ \eta_1 = \frac{\rho_{c0} - \rho_c}{\rho_{c0}},\ Le = \frac{D_{ef}}{a_c},\ \nu = \bar{\nu}\frac{\rho_g a_0}{\rho_c}.$$

Here dimensional values: a_0 – initial concentration of gaseous oxidant; ρ_{c0}, ρ_c – initial and current content of condensed substance in unit volume; ρ_g – density of gas phase; c_c – heat capacity of condensed substance; R-universal gas constant; E – activation energy of heterogeneous reaction; Q – thermal effect of heterogeneous reaction related to unit mass of oxidant, a_c – thermal diffusivity of condensed phase; D_{ef} – effective diffusivity of oxidant; $\bar{\nu}$ – amount of condensed substance reacting with 1 g of oxidant. Dimensionless variables and parameters: θ – temperature; θ_{in} – initial temperature of the sample equal to ambient temperature; η – oxidant conversion depth; η_1 – condensed substance conversion depth; $\eta_{1,\,k}$ – maximum condensed substance conversion degree; Le – Lewis parameter analog for oxidant; γ, ν – parameters.

According to the above expression, the temperature in the reaction zone increases with an increase in the effective diffusion coefficient D_{ef}, the value of which increases with an increase in the porosity of the sample [17].

In another series of experiments, the samples made of nonpassivated iron nanopowder were also pressed in argon atmosphere, however, closed weighing bottles with the samples after extraction from the box, until the beginning of the experiment, were kept in the air rather than argon. The experiments showed that the modes of interaction of samples with the air after their extraction from the weighing bottles depended on the duration t of the exposure of weighing bottles to the air. Thus, the first sample (t was less than 4 min) behaved like the samples from the first series of experiments, namely the sample was self-heated and it changed its color (see Fig. 4). The next sample, which was exposed in the weighing bottle to the air for 10 min, after extraction into the air heated up to 55 °C and did not change its color. The samples, which were exposed in the weighing bottle to the air for more than 20 min, did not heat up or change their color after extraction from the weighing bottle. Evidently, that time is sufficient for complete passivation of the sample. To test the hypothesis that the passivation involving the preservation of chemical activity, occurred rather than complete oxidation of the sample during the presence of the weighing bottle in the air, the following experiments were carried out (see Fig. 8).

The samples that did not heat up after removal out of the weighing bottle were ignited from the upper end with a tungsten spiral (Fig. 8). That local warming resulted in the propagation of a combustion wave along the sample. Since the surface of the sample changed its color during oxidation, the combustion velocity was

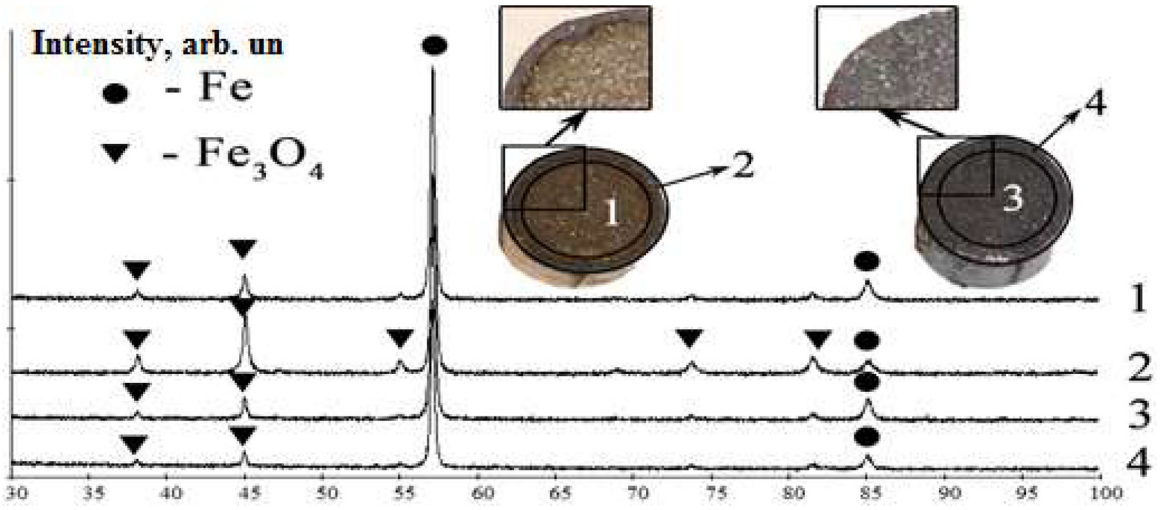

Fig. 9: X-ray patterns (pt) of the 5 mm diameter samples with of after self-heating and passivation: 1 – central part of the sample after self-heating, 2 – surface layer of the sample after self-heating, 3 – central part of the passivated sample, 4 – surface layer of the passivated sample.

determined by frame-by-frame processing of the video filming. As is seen in Fig. 8, a combustion wave propagates downward from the upper end of the sample at approximately constant velocity. Typical values of combustion velocity make 0.025 ± 0.04 cm/s.

Similar results were obtained earlier in experiments with passivated iron nanopowders [8]. It was shown that the local heating with a tungsten spiral caused the propagation of a reaction wave over the surface of the powder sample. A qualitative agreement of our results with the data [8] is an additional evidence that during the exposure of weighing bottles to the air the passivation of the samples occurred. The infrared filming of the dynamics of the change of the temperature field of the sample during propagation of the combustion wave was carried out at the same time. The video showed that the maximum temperature was almost all the time near the upper end of the sample. This result allows us to conclude that the chemical transformation process does not end in the combustion wave, and the combustion itself occurs in a superficial mode, as it was also confirmed by the X-ray analysis.

To establish the superficial mode of the air self-heating interaction for non-passivated samples and the volume one for passivated samples, the central and surface regions for each sample were analyzed separately (Fig. 9). The cross-sectional images of the samples in Fig. 9 provide an understanding of how the sample was divided into the central and surface regions. The figures in the cross-section figures correspond to the X-ray pattern.

As is seen in Fig. 9, Fe_3O_4 content in the central part of the sample (Fig. 9, pt. 1) for the samples after self-heating is significantly less than for the surface region (Fig. 9, pt. 2). These results directly indicate the superficial mode of the interaction of the samples with air during self-heating. For passivated samples, Fe_3O_4 content in the central and surface regions of the sample (Fig. 9, pt. 3, 4) is practically the same; that indicates the volume mode of the passivation process.

SEM (Ultra Plus microscope from Carl Zeiss (Germany)) study of the microstructure of the transverse fracture of a cylindrical sample after self-ignition or combustion showed that the fracture was a cluster of iron nanopowder agglomerates. Analysis of the microstructure of the individual agglomerate in the near-surface region of the sample (300–500 μm thick) revealed a porous layer ("crust") about 300 nm thick on the surface of the agglomerates. In the central part of the sample, there is no dense "crust" on the surface of the agglomerates, only a slight increase in density is observed at a depth of 100 nm. The internal structure of the agglomerates, both in the near-surface region of the sample and in the central part, has no differences and has practically the same oxygen content.

Conclusions

It is shown that the self-heating of a compacted sample made of nonpassivated iron nanopowder is not uniform, although it begins simultaneously within the entire surface of the sample. It is found that the maximum temperature of self-heating decreases with an increase in relative density of samples, which indicates that the oxidation process is limited by the diffusion supply of oxidant. It is shown that the process of interaction of samples with air occurs in a superficial mode. A qualitative agreement of the results of the theoretical analysis with experimental data is obtained. The dependence of the mode of interaction of samples with the air on the duration of the exposition of weighing bottles to the air is revealed. The possibility of passivation of compacted samples made of iron nanopowder is experimentally established.

Funding: This work was supported by the Russian Science Foundation (grant number 16-13-00013P).

References

[1] J. Bouillard, A Vignes, O. Dufaud, L Perrin, D. Thomas. *France J. Hazard. Mater.* **181**, 873 (2010).
[2] A. Pivkina, P. Ulyanova, Y. Frolov, S. Zavyalov, J. Schoonman. *Propellants, Explos. Pyrotech.* **29**, 39 (2004).
[3] M. Hosokawa, K. Nogi, M. Naito, T. Yokoyama. *Nanoparticle Technology Handbook*, Elsevier, Amsterdam, p. 157 (2007).
[4] N. M. Rubtsov, B. S. Seplyarskii, M. I. Alymov. *Ignition and Wave Processes in Combustion of Solids*, Springer international publishing, Switzerland, p. 250 (2017).
[5] M. Flannery, T. G. Desai, T. Matsoukas, S. Lotfizadeh, M. A. Oehlschlaeger. *J. Nanomater.* **2015**, 185 (2015).
[6] M. J. Meziani, C. E. Bunker, F. Lu, H. Li, W. Wang, E. A. Guliants, R. A. Quinn, Y. P. Sun. *ACS Appl. Mater. Interfaces* **1**, 703 (2009).
[7] R. Nagarajan, T. A. Hatton. *Nanoparticles: Synthesis, Stabilization, Passivation, and Functionalization*, American Chemical Society, Washington DC, p. 250 (2008).
[8] B. S. Seplyarsky, T. J. Ivleva, M. I. Alymov. *Doklady Akademii Nauk, Phys. Chem.* **478**, 310 (2018).
[9] M. I. Alymov, N. M. Rubtsov, B. S. Seplyarskii, V. A. Zelensky, A. B. Ankudinov. *Mendeleev Commun.* **26**, 452 (2016).
[10] M. I. Alymov, N. M. Rubtsov, B. S. Seplyarskii, V. A. Zelensky, A. B. Ankudinov. *Mendeleev Commun.* **27**, 482 (2017).
[11] M. I. Alymov, N. M. Rubtsov, B. S. Seplyarskii, R. A. Kochetkov, V. A. Zelensky, A. B. Ankudinov. *Mendeleev Commun.* **27**, 631 (2017).
[12] S. Dong, H. Cheng, H. Yang, P. Hou, G. Zou. *J. Phys.Condens. Matter.* **14**, 11023 (2002).
[13] E. M. Hunt, M. L. Pantoya. *J. Appl. Phys.* **98**, Paper No. 034909 (2005).
[14] F. Saceleanu, M. Idir, N. Chaumeix, J. Z. Wen. *Frontiers in Chemistry*, 00465 (2018).
[15] A. A.Gromov, U. Teipel. *Metal Nanopowders: Production, Characterization, and Energetic Applications*, John Wiley & Sons, p. 196 (2014).
[16] S. S. Kiparisov, G. A. Libenson. *Powder Metallurgy*, Metallurgy, Moscow, (in Russian), p. 235 (1991).
[17] D. A. Frank-Kamenetskii. *Diffusion and Heat Transfer in Chemical Kinetics*, Plenum Press, New York-London, p. 209 (1969).